Back-analysis of the extreme squeezing conditions in the exploratory adit to the Lyon-Turin base tunnel

G. Russo & L. Repetto
Geodata, Turin, Italy

J. Piraud & R. Laviguerie
Antea, Orleans, France

ABSTRACT: During the construction of the S.Martin La Porte access adit, 9m in diameter, extreme squeezing conditions occurred while crossing Carboniferous schistose formations, with diametric convergence up to 2m. Back-analysis of monitoring results shows that an acceptable simulation of the observed excavation behaviour can be derived using a combined analytical and numerical approach, with simple elasto-plastic laws but a progressive reduction of residual parameters and a relevant increase of dilatancy.

1 INTRODUCTION

The construction of S.Martin La Porte (SMLP), France, access and exploratory adit has been in progress since 2002, on behalf of the Franco-Italian company LTF (Lyon Turin Ferroviaire), in charge of the projected transalpine tunnel in the central part of the new railway link Lyon-Turin.

After 800 m of fair geotechnical conditions in Jurassic limestone and anhydrite, extreme squeezing conditions occurred while crossing Carboniferous schistose formations ("Houiller"). The access adit, ≈9m in internal diameter and 2.4km in length, is today close to reach the junction with the future base tunnel. However, the present paper focuses in particular on the excavation of a stretch of tunnel of about 100m, located after chainage 1+270 ("PM 1270", see Fig.1), in which the most intense deformation phenomenon occurred.
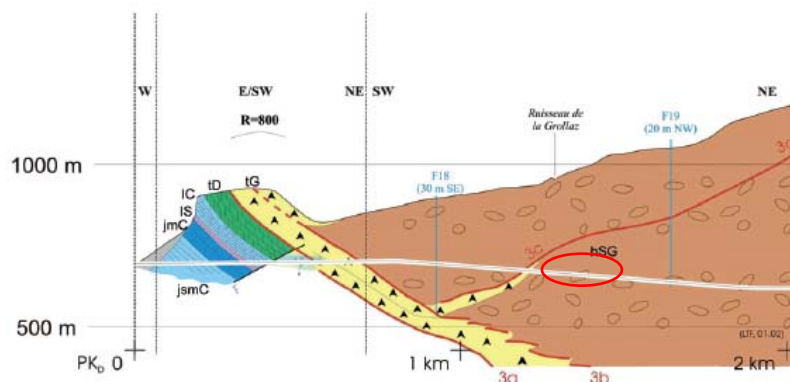

Figure 1. Geological sketch of S.Martin La Porte Adit (≈2.4km in length): the abbreviation "hSG" represents the Encombres Unit of the Carboniferous schistose Houiller Formation. The ellipse indicates the reference zone for the present paper.

In order to interpret correctly the excavation behaviour, an intensive program of monitoring has been implemented, including the measurement of convergences, plastic radius around the cavity (by means of rod and wire extensometers), tunnel face extrusion and stress in the final

lining. On the basis of such measurements and systematic geomechanical survey of tunnel face, a deepened back-analysis were carried-out by implementing either analytical and numerical methods, as well as different geotechnical modelling.

2 GENERAL SETTING

The analysis showed in the present paper was developed in the frame of the geotechnical design of the future basis tunnel. On the other side, the design and construction supervision of the SMLP adit are contractually separated from the previous studies, but, evidently, of great interest for incorporating such a practical experience in the ongoing geotechnical modelling. As a consequence, the starting point for back-analysis of the SMLP adit is the set of parameters hypothesized for the geotechnical design of the basis tunnel, while crossing the same rock mass (Fig. 2).

Figure 2. Example of appearance of the graphitic schists of Houiller at the tunnel face.

As reported by Rettighieri et al. (2008), the excavation of the adit has been realised by conventional method, the section of excavation (Fig. 3) was about 94m^2 (radius R=5.4m) and the systematic stabilisation measures included:
In advancement to the excavation:
• pre-reinforcement of tunnel face by cemented fibreglass elements (each 10m: n.40, L=16m);
Radial stabilisation measures (1m round):
• 10cm of shotcrete on face and cavity;
• n.10 Swellex MN12 in the crown;
• n.34 self-boring bolts (L=8m);
• sliding steel ribs (TH44/58);
• protective steel mesh
and, at distance, when stabilization occurred, final lining of plain concrete.
The resulting average advance rate was about 0.5m/d, with maximal value of 1.5m/d.
The design described above was not resulting in the expected equilibrium condition: in presence of about 300-330m of overburden, more than 2m of convergence was finally measured, causing the complete crushing of the primary support and the consequent necessity of reshaping of the cavity (Fig. 4). In addition, the load on the final lining was not reaching an equilibrium condition, as well.
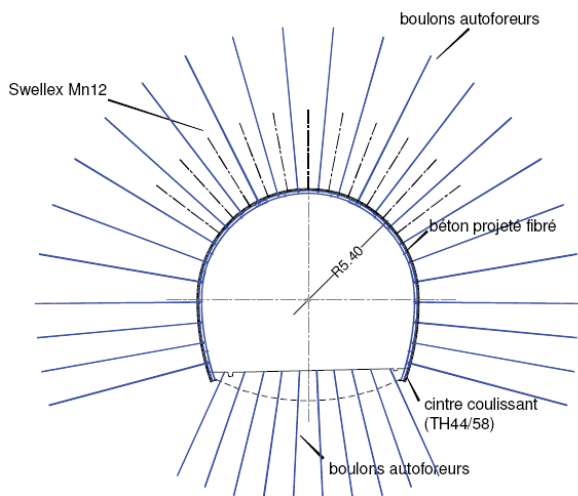In the next section, a summary of monitoring is reported.

Figure 3. Stabilization measures applied (Rettighieri et al., 2008).

Figure 4. Imagine of the deformed excavation section and of the enlarged one after re-shaping.

3 MONITORING

3.1 *Convergence measurements*

Till the time when the back-analysis reported in this paper was made, the monitoring did not confirm an equilibrium condition, neither in terms of convergences, nor in term of stress in the lining realized in the re-shaped sections. In Fig. 5, a synthesis of the convergence measurements vs time is reported.
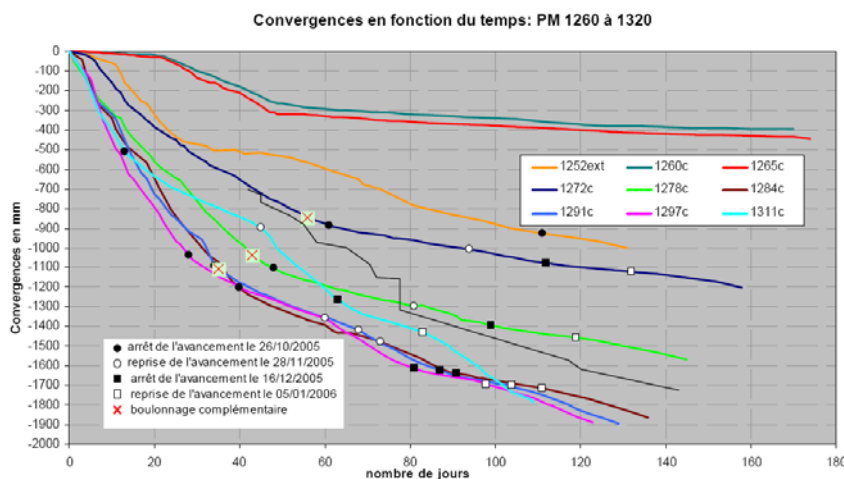

Figure 5. Synthesis of the convergence measurements vs time (days after excavation) between PM 1260-1320m. Note: see the comment in the text about the measurements at PM1260-1265.

From Figure 5, the following is derived:
- in some cases the measured convergences are exceeding 2m after more than 120 days from the excavation and with distance between 55 and 110m from the tunnel face;
- for the sections between PM1284 and PM1297, the mean gradient in the first 20 days is in the order of 35-40mm/d;

- some additional explanations are necessary for the measurements at PM1260÷1265: here, a cave-in occurred and a plain concrete lining was immediately realized to stabilize the section, but additional failures occurred before of closing the invert (Figs. 4 and 9).

3.1.1 *Extensometer measurements*

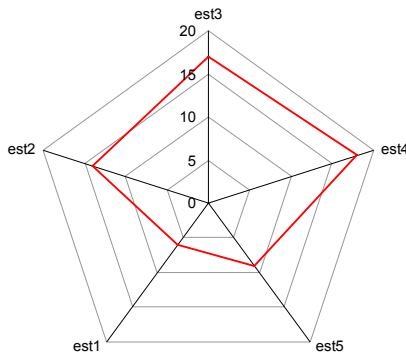The evolution of plastic zones around the cavity was monitored by extensometers.

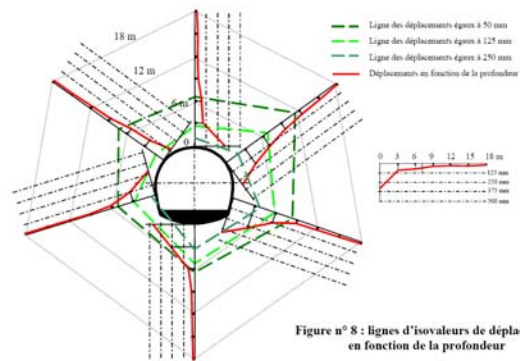Figure 6. Estimation of plastic zone thickness at PM1330.

Figure 7. Iso-displacement lines beyond the contour of excavation at PM1330.

The graphs of Figures 6 and 7, show some dissymmetry with a larger extension of the plastic zone on the right of the section, where about 17-18m are reached. Such a dissymmetry, confirmed also by the radial displacements of the cavity, is likely to be linked with the anisotropy of rock mass and local state of stress.

3.1.2 *Measurements of the tunnel face extrusion*

The control of the face extrusion, as well as the development of plastic zone ahead of the tunnel face, was realised by incremental extensometers. Figure 8 shows the progressive increase of the face extrusion with the progress of excavation. In particular, the case refers to the max measured extrusion (about 20cm), before a relevant reduction of the deformation at about PM 1355, where a higher presence of meta-sandstones was observed at the excavation face, resulting in 4-5cm of total face extrusion.

The analysis of displacements allows to estimate that, in the presence of the described pre-reinforcement of the face by fibreglass elements, plastic zone is developing about 5m in advance to the excavation, i.e. more or less one radius of the tunnel.
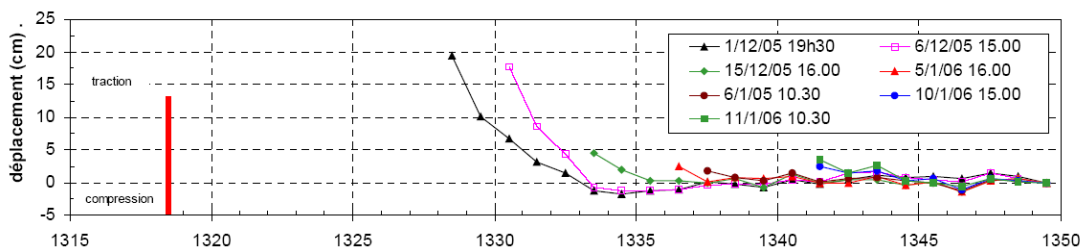

Figure 8. Measurement of the tunnel face extrusion.

3.1.3 *Stresses in the lining*

As already remarked, special conditions have occurred in the stretch of tunnel between about PM1260-1265, pointed out by failures of the immediate support and the consequent necessity of installation of additional stabilisation measures (like tendons, etc., Fig. 9)

Figure 9. Heavy structural damage near the crown at PM1260.

Figure 10. Tangential stress inferred from strain measurements at PM1230 (cross: flat jack measurements).

The progressive increase of stress in the lining was also measured in other sections, after the re-shaping illustrated in Figure 9. For example, in Figure 10, the increase of stress up to more than 10MPa is observed for the monitoring section at PM1230.

4 BACK-ANALYSIS

The tunnel excavation behaviour is the result of a complex interaction between the rock mass and the construction process. Given the number of parameters and the related uncertainties, it is probable that different combinations of values may determine a similar result. For example, in the examined case, a relevant factor on the resulting behaviour may be the eventual influence of the rock mass and/or in-situ stress anisotropy.

Two steps of analysis were developed:
• in the first time analytical methods and homogeneous/isotropic conditions were considered for a general setting (§4.1);
• then a more detailed verification has been performed by numerical methods and with reference to either an isotropic and anisotropic modelling. (§4.2).

4.1 *Step 1: general setting by analytical methods*

For getting a first overview of the tunnel behaviour, analytical methods are used with some simplified assumptions:

Figure 11. Example of geological mapping of tunnel face showing the high rock mass tectonization.

• The rock mass is "globally" homogeneous and isotropic;

• the in-situ state of stress is also isotropic and proportional to the depth of the tunnel.

Considering the rock mass structure revealed from face mapping (Figure 11), highly variable and locally also chaotic, it is believed that such assumptions are reasonable.

The establishment of a framework has contemplated a comparison between:

• Convergence of the cavity elaborated according to the method of Sulem et al. ("Sulem", 1983 and subsequent);

• convergence of the cavity calculated with the design parameters using the Convergence-Confinement method (CC).

4.1.1 *Analysis of radial convergences*

The basic formulation of the Sulem's method is:

$$C(x,t) = C(\infty, x)\left[1 - \left(\frac{X}{x+X}\right)^2\right]\left[1 + m\left(1 - \left(\frac{T}{t+T}\right)^n\right)\right] \quad \text{where:} \tag{1}$$

- x = distance from the excavation face (x=Va×t where Va is the advance rate and t is time; t = 0 corresponds to the passing of the face at the section under analysis);
- X = characterize the distance of influence of the excavation face (≈4X): in general it is assumed to be equal to 0.84×Rp where Rp is the radius of the plastic zone;
- T = characteristic time which determine the rheological properties of the rock mass;
- C(∞,x) = instantaneous convergence at infinite distance and time; it is equivalent to the convergence that would occur under the hypothesis of Va=∞ and therefore it is comparable with that calculated from the convergence-confinement method;
- C(x,t) = is the convergence at time t and distance x from tunnel face;
- m = represents the increment of the instantaneous deformation due to the effect of rheology;
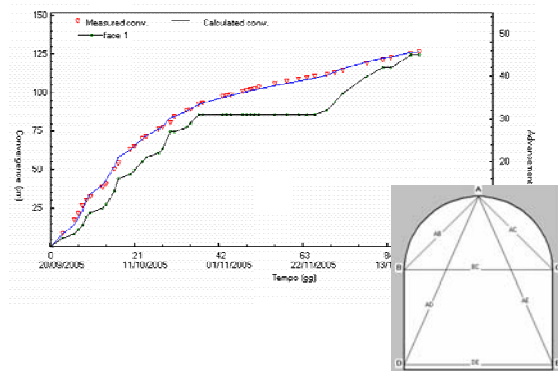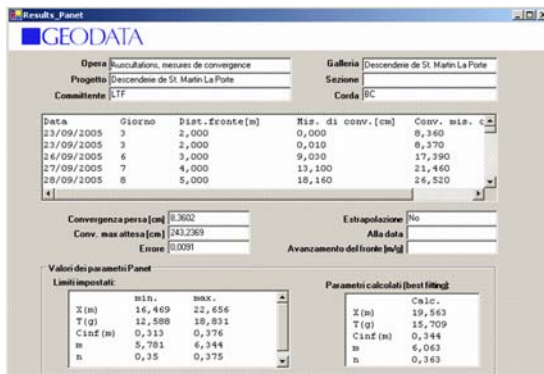- n = constant (often ≈0.3).

Figure 12. Example of best-fitting convergence analysis.

The measurements of convergence have been analyzed deriving the Sulem's parameters (Fig. 12 and Table 1).

Table 1. Example of Sulem's parameters derived by analyzing the convergence measurements.

Section	X (m)	T (days)	C∞x (m)	m	n	C lost (m)	C∞x(1+m) (m)
1272	32	41	0.34	4.1	0.45	0.04	1.75
1278	29	16	0.19	9.2	0.41	0.03	1.91
1284	29	28	0.41	6.6	0.48	0.10	3.10
1291	20	16	0.34	6.1	0.36	0.08	2.43
1297	22	63	0.44	10.6	0.39	0.04	5.07
1322	103	106	0.53	11.7	0.63	0.06	6.75

Note: C lost = convergence already occurred ("lost") before the first measurement.

From Table 1 the following is derived:

- the results at PM1322 appear different (in particular X and T) from other sections, for which:
- the influence of tunnel face (=4X) ranges between about 75 and 125m;
- the characteristic rheological time T varies between 16 and 63days;
- the instantaneous convergence (C∞,x) is between 0.19 and 0.44m;
- the "lost" convergence at tunnel face ranges between 0.03 and 0.10m;
- the theoretical final convergence [C∞x(1+m)] is 5÷10 times the instantaneous one (≥2m).

4.1.2 *Analysis of instantaneous behaviour by Convergence-Confinement method*

According to the ongoing geomechanical study for the Base Tunnel, the characterization associated to graphitic schists and sandstones of the Houiller (Encombres Unit) is presented in Table 2.

Table 2. Rock mass geomechanical properties (base reference for back-analysis).

	Scenario→	unfavourable	most likely	favourable*
	Geomechanical groups (GG)→	G9	G8	G6
H&B intact rock constant m_i		7	7	8
Intact rock strength σ_c (MPa)		20	20	45
Geological Strength Index GSI *[GSIres]*		20-30 *[20-25]*	30-40 *[25-25]*	40-50 *[25-25]*
Deformability modulus E_d (GPa)		0.7-1.6	1.6-4.0	4.0-9.3

Notes: * associated to local high presence of meta-sandstone layers; H&B=Hoek and Brown; GSIres=GSI reduced value for calculating residual rock mass parameters.

In Figure 13 and Table 3 the characteristic lines for the G8 and G9 geomechanical groups (C. Carranza T. solution, 2003-2004) and the results for G8 are reported, respectively, for the overburden H=300m.
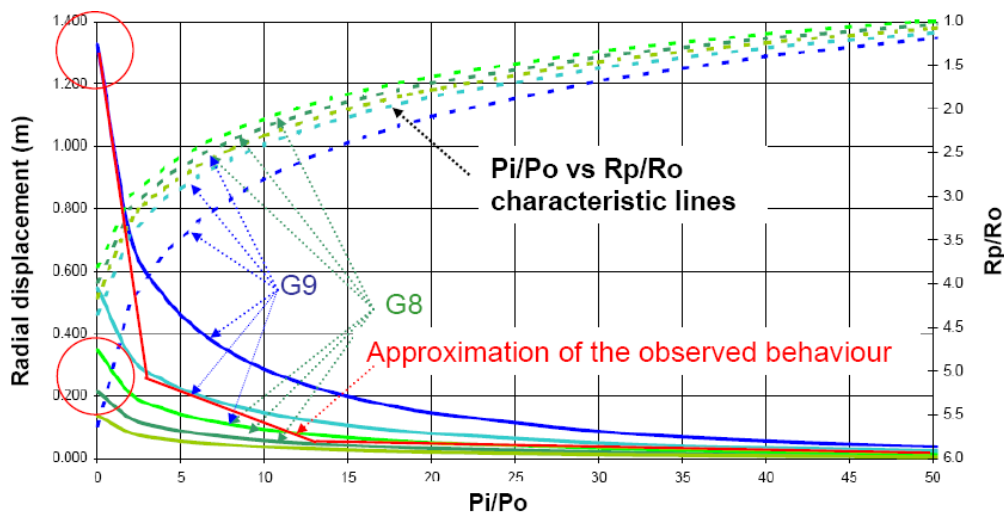

Figure 13. Pi/Po vs Radial displacement and Pi/Po vs Rp/Ro curves for G8 and G9.
Notes: Pi/Po = internal/lithostatic pressure; Rp/Ro=plastic/equivalent radius. The circles show the correspondence with the instantaneous (lower) and total (upper) displacements derived by Sulem's method.

Table 3. Results of the analysis by characteristic lines for G8 and comparison with the instantaneous convergence derived by Sulem method. Note: uo=radial displacement at tunnel face.

G8 parameters→		min		mean		max	
dilatancy ψ	(°)	ψ=0	ψ=5°	ψ=0	ψ=5°	ψ=0	ψ=5°
final displacement uf	(m)	0.31	0.38	0.19	0.24	0.12	0.15
C∞,x = 2(uf-uo)	(m)	0.48	0.60	0.30	0.38	0.19	0.24
C∞,x (Sulem)	(m)	0.44		0.34		0.19	

By comparing Table 2 and Table 3, the following is derived:
- the radial displacements for G8 calculated by CC are generally consistent with the instantaneous convergences derived by Sulem's method;

- the radial displacement for G9 calculated by CC are comparable to the final total convergences, i.e. comprehensive of the time-dependent component, derived by Sulem's method.

Consequently:

- for modelling of the rock mass till the opening up of the excavation face, it is considered adequate to use the G8 (most likely) parameters;
- for the simulation of the successive excavation behaviour, in which time-dependent deformations are prevalent, it is necessary to decay the parameter values in the plastic zone around the cavity.

It should be noted that the eventual reference to pessimistic rock mass parameters (for example as G9), does not appear consistent with the observed excavation behaviour at tunnel face, even considering face reinforcement.

4.1.3 *Integrating the Convergence-Confinement and Sulem methods*

A satisfactory representation of the observed behaviour is derived by integrating the CCm and Sulem methods. In particular, to the instantaneous displacements calculated by CCm, the rheological component obtained by Sulem method is added, for different advance rates of excavation (Figure 14). This is done by referring to the relative longitudinal profile of deformation[1]
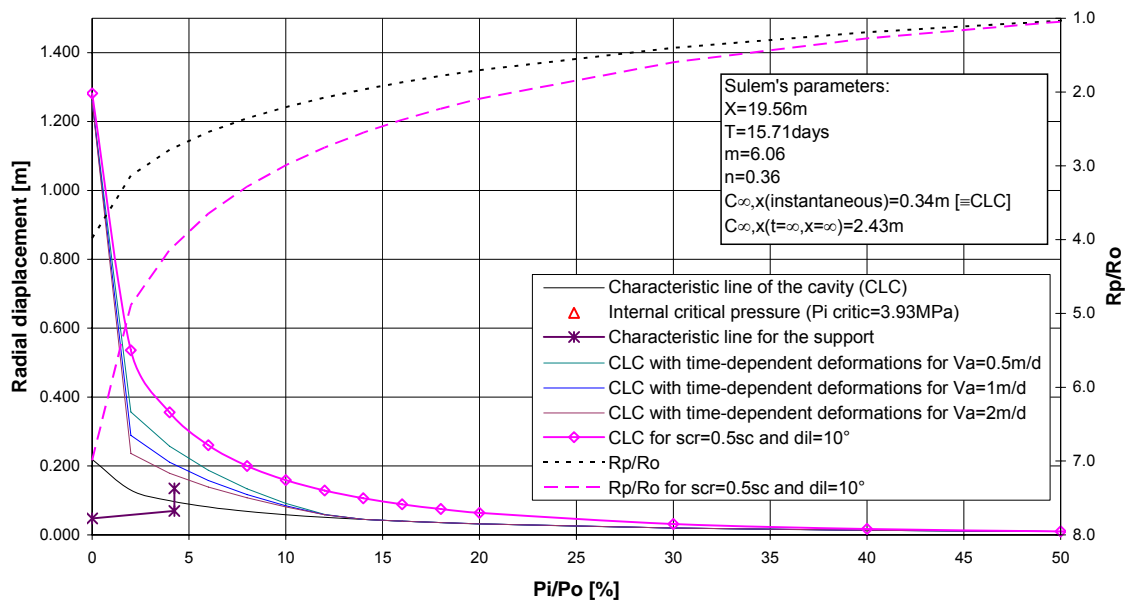

Sulem's parameters:
X=19.56m
T=15.71days
m=6.06
n=0.36
C∞,x(instantaneous)=0.34m [≡CLC]
C∞,x(t=∞,x=∞)=2.43m

Legend:
— Characteristic line of the cavity (CLC)
△ Internal critical pressure (Pi critic=3.93MPa)
—✳— Characteristic line for the support
— CLC with time-dependent deformations for Va=0.5m/d
— CLC with time-dependent deformations for Va=1m/d
— CLC with time-dependent deformations for Va=2m/d
—◆— CLC for scr=0.5sc and dil=10°
······ Rp/Ro
– – – Rp/Ro for scr=0.5sc and dil=10°

Figure 14. "Integrated" characteristic lines for G8: instantaneous and total (including time-dependent deformation) curves for different advance rates of excavation (0.5-1.0-2.0m/d); a first attempt of simulation of the observed behaviour by increasing dilatancy and reducing residual parameters values, is also reported (see curve with symbols).

4.2 *Step 2: Numerical verification*

For the numerical verification of the observed behaviour, reference has been done both to an equivalent-continuum and isotropic geotechnical model (A) and to a pseudo-discontinuum and anisotropic one (B), by considering ubiquitous joints. Both plane and axisimmetric analysis have been performed using FLAC 5.0 code (Itasca). According to the previous section, rock mass "softening" has been simulated by gradually reducing deformability and shear strength, as well as dilatancy, up to reproducing the observed behaviour.

---

[1] The equation ur/uf=(1+exp(-x/2))$^{2.2}$ is used in the case, as derived by axisimmetric analysis; such an equation is quite similar to the one proposed by Hoek (1999).

4.2.1 *Equivalent-continuum isotropic modelling (A)*

In Table 4 and Figure 15, a synthesis of both the procedure applied and the relative results is presented for the modelling of Type A.

Table 4. Synthesis of numerical analysis by FLAC 5.0 ("A" model).

Step	x (m)	λ	ψ	E_d/E_{do}	$\sigma_{cmr}/\sigma_{cmr0}$	ur (m)	Spl(m)
0	0	0.82	0 (K=1)	1.0	1.0	0.05	5
1	1-2	0.95	0 (K=1)	1.0	1.0	0.15	10
2	10	0.99	$\psi=\varphi_r$	0.8	1.0	0.38	12
3	>100	1.00	(K>1)	0.4	0.8	1.2-1.3	15-16

Notes: x=distance from the face; λ= deconfinement =(1-Pi/Po); ψ= angle of dilatancy; K= dilatancy factor= (1+sen(ψ (σ3))/(1-sen(ψ(σ3))); E_{do}=deformability modulus; E_d=reduced ("softened") deformability modulus; φ_r = residual friction angle; σ_{cmr0}= residual rock mass strength; σ_{cmr}= "softened" residual rock mass strength; ur= radial displacement; Spl= thickness of plastic zone.
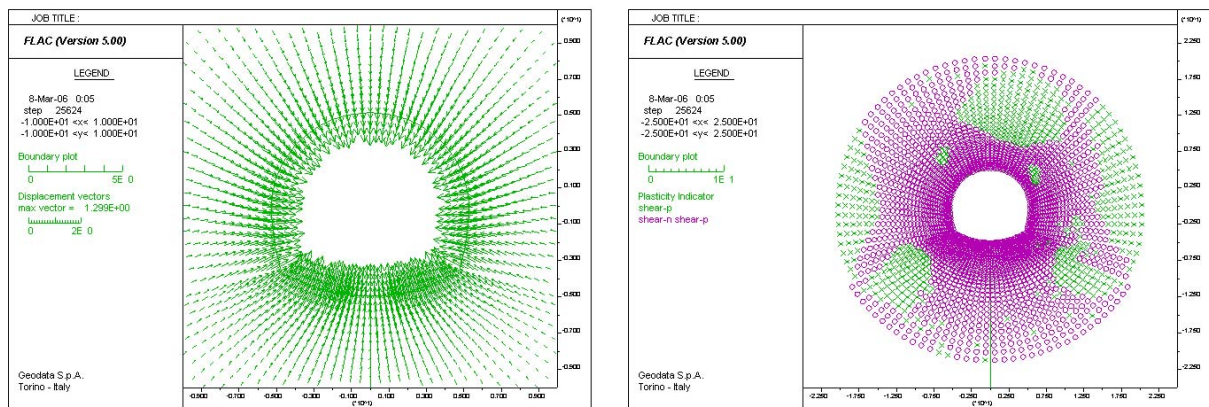

Figure 15. Type A modelling: radial displacement and plastic zone.

4.2.2 *Pseudo-discontinuum anisotropic modelling (B)*

For simulating rock mass anisotropy, ubiquitous joints have been modelled according the observed rock mass structure and the Jaeger and Cook (1969) failure criterion has been adopted.

In particular, as reported in Figure 16, the shear strength σj of the discontinuities of Houiller (Encombres Unit) has been considered, as well as, for rock mass matrix, the equivalent rock mass strength σcm such that (σcm+ σj)/2 ≈ σcmG8 (i.e. the G8 rock mass strength).
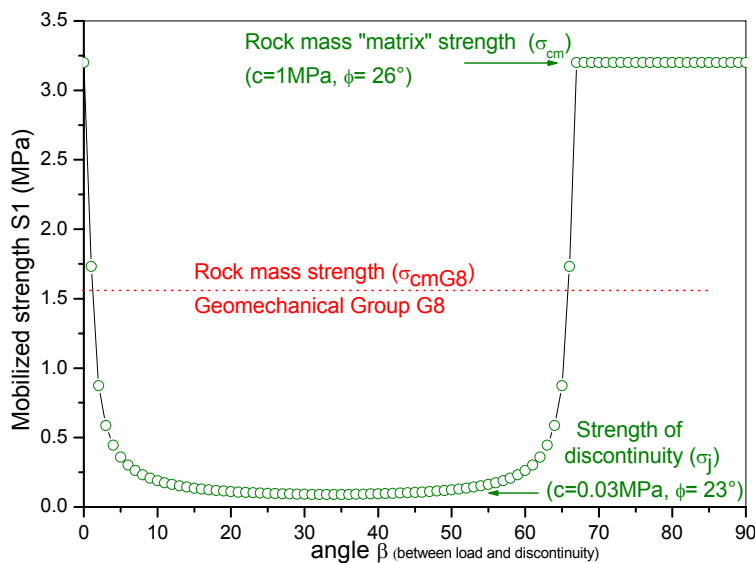

Figure 16. Jaeger and Cook failure envelope for Type B modelling.

In Table 5 and Figure 17, a synthesis of both the procedure applied and the relative results is presented for the modelling of type B. See also Figure 18 for a practical comparison with the observed behaviour at excavation.

Table 5. Synthesis of numerical analysis by FLAC 5.0 ("B" model).

Step	x (m)	RM	J	λ	ψ	Ed/Edo	cr/c	ur (m)	Spl (m)
0	0	c=1MPa; φ=26° E=1645MPa ν=0.3	cj=0.03MPa; φj=23° cjr=0; φjr=23°	0.82	0 (K=1)	1.0	1.0	0.05	2-3
1	1-2			0.95	0 (K=1)	1.0	1.0	0.18	7-8
2	10			0.99	ψ=φ$_r$	0.8	1.0	0.3	9-10
3	>100			1.00	(K>1)	0.4	0.5	1.2-1.3	12-13

Notes: RM = rock mass "matrix" parameters; J= joint parameters; c= cohesion, cr=reduced cohesion; for other symbols see Table 4.
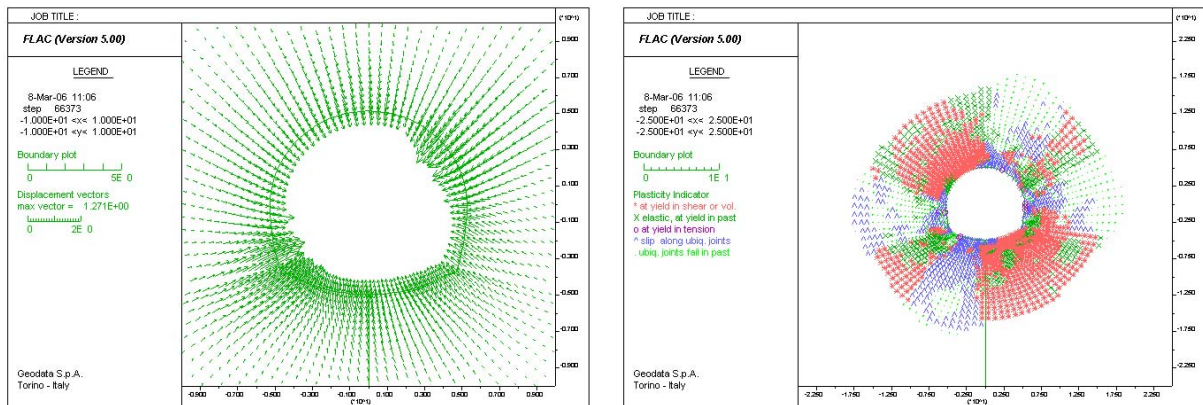

Figure 17. Type B modelling: radial displacement and plastic zone.

Figure 18. Deformations of the excavation contour of SMLP adit: see Figure 17 for comparison.

4.3 *Interpreting the results*

Both the isotropic and the anisotropic models permit a reasonable simulation of the observed excavation behaviour, in terms of both radial displacements and development of the plastic

zone, thus confirming the validity of the formulated hypotheses. Consequently, the following comments are added:
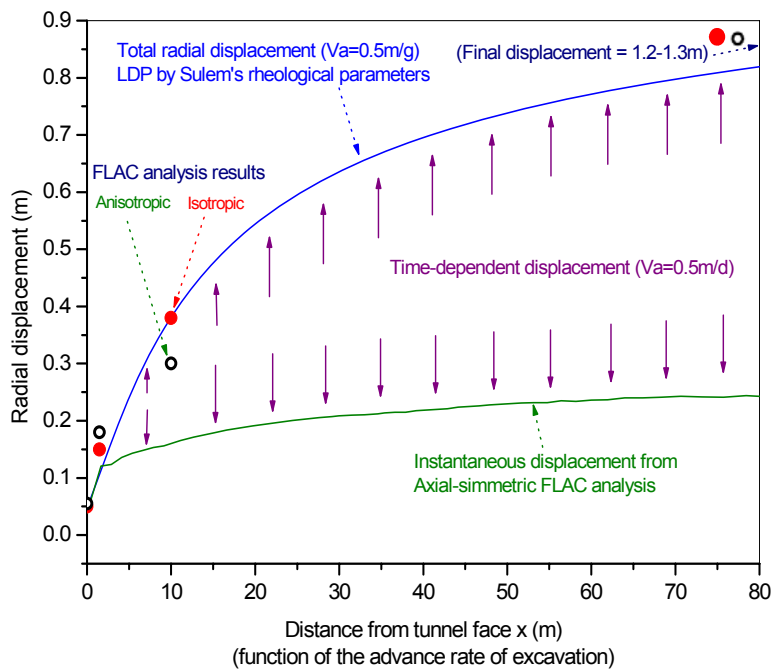

Figure 19: Comparison of numerical analysis results and longitudinal deformation profiles

- the large deformations observed in SMLP adit could be linked to a combined effect between a markedly dilatant behaviour of the rock mass and viscous/ weathering phenomena;
- in a similar way to previous observations in structurally-complex formations of the Italian Appenines, the rapid decompression related to the excavation, is suspected to determine a progressive failure of the structural bonding ("between the scales") of the schistose rock mass with significant volume increase.

In such a squeezing ground, the support concept adopted (i.e. "max deformations→max stress release→optimal equilibrium condition") does not yield the expected result; on the contrary, the design approach lead in the case to:

- progressive de-structuring of plasticized rock mass, with decay of residual properties ("softening");
- increase of rock mass permeability and consequent (probable) attraction of groundwater from the surrounding;
- notable additional deformations;
- dispatching of portions of rock in the plastic zone with consequent mobilization of additional gravitational loads on the support;
- impossibility to reach an equilibrium condition even with the complete release of original stress and after convergences of the order of several meters.

5 FURTHER DEVELOPMENTS AND CONCLUSIVE REMARKS

The back-analysis of monitoring results shows that an reasonable/acceptable simulation of the observed excavation behaviour can be derived using a combined analytical and numerical approach of modelling. Despite an evident time-dependent rock mass behaviour, the reference to simple elasto-plastic laws provide satisfactory results by considering an adequate progressive reduction of the residual geomechanical parameters and together a relevant increase of dilatancy.

However, it is evident that more sophisticated and detailed elasto-visco-plastic analyses have higher chances to reproduce faithfully the complex deformation phenomenon, despite some

concern may arise about the reliability of the key time-dependent parameters. Anyway, very good results have been reported by Regazzoni (2006) and Rettighieri et al. (2008), by applying two different time-dependent constitutive models, i.e. the CVISC (Itasca, 2006) and SHELVIP (Debernardi, 2008), respectively.
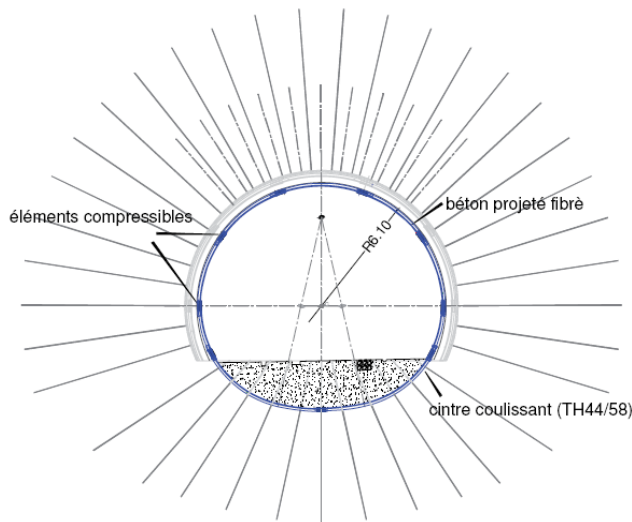

Figure 19. New section type adopted for managing squeezing in the SMLP adit (Rettighieri et al., 2008).

Rettighieri et al. (2008) report also a detailed description of the successive design developments for managing the extreme squeezing conditions encountered in the SMLP adit.

In addition to making the section as circular as possible and the pre-reinforcement of the tunnel face, the following schemes have been finally adopted (Fig. 19) with satisfactory results:
a) at the tunnel face: "high deformable" support system based on bolts and sliding steel ribs;
b) at about 30m: "medium stiff" support based on steel ribs and shotcrete shell which includes n.9 decompression joints filled with compressible concrete precast elements;
c) at about 80m, "final stiff support" consisting on 1m of plain concrete lining.

REFERENCES

Carranza-Torres, C. 2003. *Computation of stress and displacement distributions around circular opening subject to symmetrical loading in elasto-plastic Mohr-Coulomb and Hoek-Brown materials.* Personal communication.
Hoek, E., Carranza-Torres, C., & Corkum, B. 2002. 2002 (ed.), *Hoek-Brown failure criterion; Proc.North American Rock Mechanics Society*, Toronto, July 2002.
Jaeger, J.C. & Cook, N.G.W. 1969. *Foundamental of Rock Mechanics*. London: Chapman and Hall.
Regazzoni, P. (2006): *Les ouvrages souterrains, modélisation du comportement différé: Application à la discenderie de S.Martin La Porte*. Rapport final de stage pour le Projet de Fin d'études. Grenoble: Université Joseph Fournier.
Rettighieri, M., Triclot, J., Mathieu, E., Barla, G. & Panet, M. 2008. *Difficulties associated with high convergences during excavation of the Saint Martin La Porte access adit; Congrès International de Monaco.* Monaco: AFTES.
Sulem, V., Panet, M., Guenot, A. 1987. Closure analysis in Deep Tunnels. *Int. Jour. Rock Mech. Min. Sc. & Geom. Abstr.* 24(3): 145–154.